Journal of Ceramic Processing Research. Vol. 9, No. 4, pp. 430~436 (2008)

J O U R N A L O F
Ceramic Processing Research

Characteristic evaluations of microwave absorbers using dielectric and magnetic composite materials

Young Joon An[a,*], Ken Nishida[a], Takashi Yamamoto[a], Shunkichi Ueda[b] and Takeshi Deguchi[b]
[a]*Dept. of Communications Engineering, National Defense Academy, Yokosuka, 239-8686 Japan.*
[b]*Osaka Laboratory, Tayca Co., Osaka, 551-0022 Japan*

A microwave absorber for use in an electronic toll collection(ETC) device, having a central frequency of 5.8 GHz, is fabricated using a composite of magnetic (iron, Fe (coated by Fe_3O_4), made from Carbonyl Iron, $Fe(CO)_5$) and dielectric (titanium oxide, TiO_2) material. The reflection loss in free space, using a circularly polarized wave, was −20 dB or more around a central frequency of 5.8 GHz at incident angles of up to 60°, which satisfies the necessary conditions for ETC use in JAPAN.
In this study, we explain the characteristic evaluations of microwave absorbers by changing the weight ratio of Fe/TiO_2 composite materials (Fe/TiO_2 = 100/0-0/100) and incidence characteristics of the transverse electric wave (TE wave), the transverse magnetic wave (TM wave) and the circularly polarized wave (CP wave) in a free-space without a characteristic deterioration. In addition, we show the experimental results by changing the arrangement of microwave absorber that also satisfied a necessary condition for ETC use.

Key wards: Microwave absorber, Complex permittivity, Complex permeability, Dielectric-magnetic composite material.

Introduction

In recent years, wireless technology has progressed rapidly. To enable the processing of more information at high speed, the transmission frequency has been shifted toward a high-frequency domain. Frequency classification in Japan, according to the field of application, is given as follows: cellular phone; 800 MHz to 2 GHz, millimetre wave wireless local area network (LAN); 2.45 and 5.2 GHz, electronic toll collection (ETC); 5.8 GHz and intelligent transport system (ITS); 76 GHz. The radiation of electromagnetic waves in free space has increased, because of these various applications, and there is concern about the effects on other electronic devices. For example, there is the uncontrollable starting or unexpected stopping of a machine, which has been well known for many years [1]. For those reasons, the development of microwave absorber is necessary to improve the electromagnetic wave environment.

In this report, we propose new materials for microwave absorbers, in which these materials are composed of magnetic (iron coated by Fe_3O_4, made from carbonyl iron, Fe $(CO)_5$) and dielectric (titanium oxide, TiO_2) composite materials. These composite materials are applied in the design of a microwave absorber which makes reflection losses and the central frequency for a purpose, for example, the necessary conditions of ETC (5.8 GHz) use in Japan [2, 3]. Additionally we show the experiment results by changing the arrangement of the microwave absorber.

*Corresponding author:
Tel : +81-46-841-3810(Int2586)
Fax: +81-46-844-5911
E-mail: g45073@nda.ac.jp

Theory

Measurement of complex permittivity, ε_r* and and permeability, μ_r* for composite material

As shown in the schematic in Fig. 1(a), when a transverse electromagnetic (TEM) wave is vertically incident on a specimen inserted in a co-axial wave-guide, it is possible to treat the phase relations of the transmitted and reflected waves as depicted in Fig. 1(b), where $\dot{Z}c$ is the characteristic impedance, $\dot{\gamma}$ is the propagation constant, and d is the thickness of the specimen. When the reference plane is at positions indicated as planes 1 and 2, the reflection and transmission coefficients of the TEM wave, are assumed to be $\dot{S}_{11}$' and $\dot{S}_{21}$', the reflection coefficient, $\dot{S}_{11}$, and transmission coefficient, $\dot{S}_{21}$, with a specimen are given by: [4, 5]

$$\dot{S}_{11} = \dot{S}_{11}' e^{-2j\phi_1} \tag{1}$$

$$\dot{S}_{21} = \dot{S}_{21}' e^{j(\phi_1+\phi_2)} \tag{2}$$

Using Eqs.(1) and (2), the $\dot{Z}c$ and $\dot{\gamma}$ are derived as:

$$\dot{Z}c = \pm\frac{\sqrt{(1-\dot{S}_{11}^2+\dot{S}_{21}^2)^2-4\dot{S}_{21}^2}}{(1-\dot{S}_{11})^2-\dot{S}_{21}^2}, \quad \mathrm{Re}Zc\geq 0 \tag{3}$$

$$\dot{\gamma} = -\frac{1}{d}\left(log\frac{1-\dot{S}_{11}^2+\dot{S}_{21}^2-\{(1-\dot{S}_{11})^2-\dot{S}_{21}^2\}\dot{Z}c}{2\dot{S}_{21}}+2n\pi\right) \tag{4}$$

where n is an integer. Using these equation, complex permittivity, ($\varepsilon_r^* = \varepsilon_r' - j\varepsilon_r''$) and permeability, ($\mu_r^* = \mu_r' - j\mu_r''$) are calculated by:

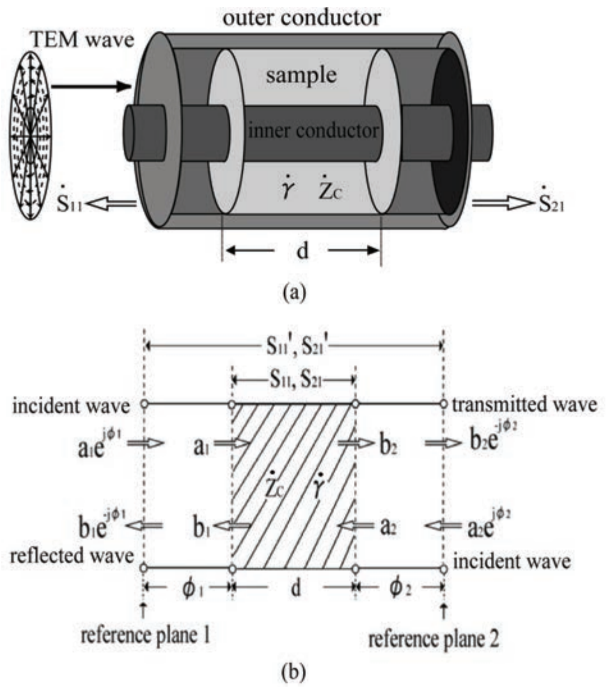

Fig. 1. (a) Schematic figure for the specimen holder inserted in a co-axial wave guide and (b) phase relations among reflected and transmitted wave and a specimen.

$$\mu_r^* = \mu_r' - j\mu_r'' = -j\frac{\lambda_0}{2\pi}\dot{Z}c\dot{\gamma} \tag{5}$$

$$\varepsilon_r^* = \varepsilon_r' - j\varepsilon_r'' = -j\frac{\lambda_0}{2\pi}\frac{\dot{\gamma}}{\dot{Z}c} \tag{6}$$

Measurement of microwave absorber

In order to obtain the frequency characteristics of a reflection loss, Γ_{11}, in a free space of the single-layer microwave absorber, the measured ε_r^* and μ_r^* are used. As expressed in the form containing ε_r^* and μ_r^*, the characteristic impedance, $\dot{Z}c$, and propagation constant, $\dot{\gamma}$, are described by:

$$\dot{\gamma} = j\frac{2\pi}{\lambda_0}\sqrt{\mu_r^*\varepsilon_r^*} \tag{7}$$

$$\dot{Z}c = \sqrt{\frac{\mu_r^*}{\varepsilon_r^*}} \tag{8}$$

When the terminal is short circuited (described as $\dot{Z}_L = 0$), the normalized impedance, $\dot{Z}_{in}$, with a specimen is given by:

$$\dot{Z}_{in} = \dot{Z}c \tanh \dot{\gamma}\, d \tag{9}$$

$$\dot{S}_{11} = \frac{\dot{Z}_{in} - 1}{\dot{Z}_{in} + 1} \tag{10}$$

$$\Gamma_{11} = 20\log \dot{S}_{11} \tag{11}$$

When the incident and reflected electrical field, $\dot{E}_i$ and $\dot{E}_r$, and magnetic waves, $\dot{H}_i$ and $\dot{H}_r$, enter vertically to the incident plane with an arbitrary angle, θ_i, in the reflection plane as shown in Figs. 2(a) the transverse electric wave (hereafter called the TE wave) and 2(b) the transverse magnetic wave (hereafter called the TM wave), the propagation constant, $\dot{\gamma}$, which is the same in both cases of the TE and TM waves, is given as:

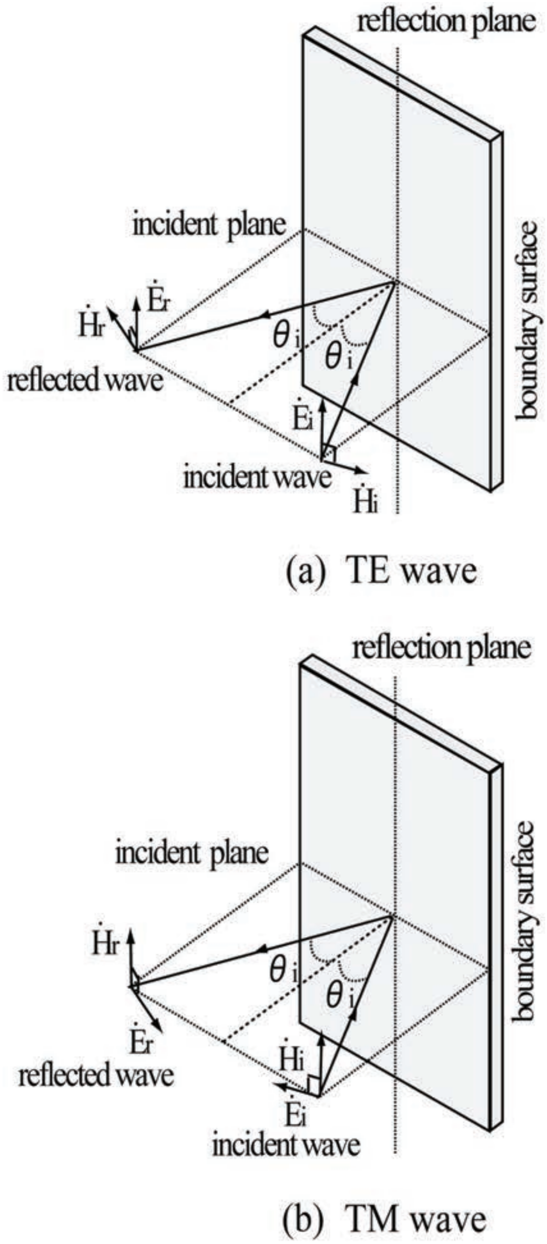

Fig. 2. Relations between incident and reflected electrical field $\dot{E}_i$ and $\dot{E}_r$, and magnetic field, $\dot{H}_i$ and $\dot{H}_r$, for (a) TE wave, and (b) TM wave.

$$\dot{\gamma} = j\frac{2\pi}{\lambda_0}\sqrt{\mu_r^*\varepsilon_r^* - \sin^2\theta_i} \tag{12}$$

Moreover the characteristic impedance, $\dot{Z}c$, and the reflection losses, Γ_{11}, of the TE and TM waves are given as:

$$\dot{Z}c = \frac{\mu_r^*}{\sqrt{\mu_r^*\varepsilon_r^* - \sin^2\theta_i}} \quad (TE) \quad (13)$$

$$\Gamma_{11} = 20\log\left|\frac{\dot{Z}_{in} - 1/\cos\theta_i}{\dot{Z}_{in} + 1/\cos\theta_i}\right| \quad (TE) \quad (14)$$

$$\dot{Z}c = \frac{\sqrt{\mu_r^*\varepsilon_r^* - \sin^2\theta_i}}{\varepsilon_r^*} \quad (TM) \quad (15)$$

$$\Gamma_{11} = 20\log\left|\frac{\dot{Z}_{in} - \cos\theta_i}{\dot{Z}_{in} + \cos\theta_i}\right| \quad (TM) \quad (16)$$

A circularly polarized wave (hereafter called the CP wave) can be expressed as a synthetic wave of two linear polarized waves, TE and TM waves, which intersect perpendicularly in a free space. Supposing an incident wave is composed of a linear polarized wave with amplitude, E_0, which has an electrical field component in the X and Y axes, the CP wave is described as: [6, 7]

$$\dot{E} = E_0\left\{\hat{x}e^{j\omega t} + \hat{y}e^{j\left(\omega t - \frac{\pi}{2}\right)}\right\}e^{-jkz} \quad (17)$$

where Eqs. (17) is expressed as the CP wave with a right wheel and the synthetic electrical field rotates in the clockwise direction. Supposing the CP wave is composed of TE and TM waves in which the phase is progressed by $\pi/2$ and the reflection loss of the TE and TM waves is denoted as $\dot{S}_{TE}$ and $\dot{S}_{TM}$, the reflection loss of CP wave is expressed as the reflection loss with the same phase and reverse phase, $\dot{S}^e$ and $\dot{S}^o$, and the reflection loss of the TE and TM waves is given as:

$$\dot{S}_{TE} = \dot{S}^e + \dot{S}^o \quad (18)$$

$$\dot{S}_{TM} = \dot{S}^e - \dot{S}^o \quad (19)$$

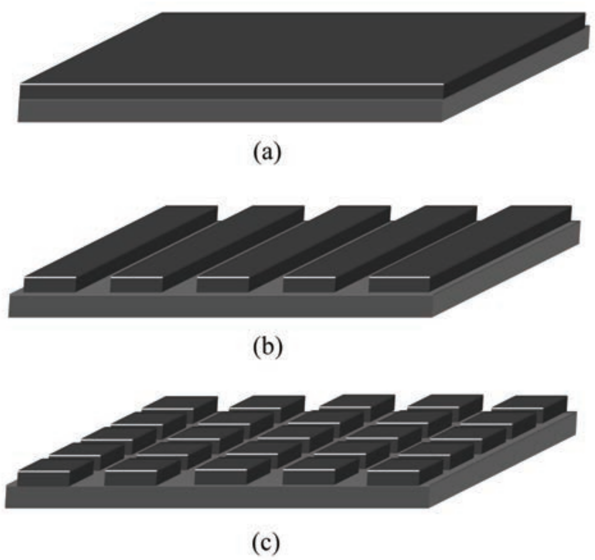

Fig. 3. Sample structure of free-space method for (a) ALL, (b) STRIPE and (c) PATTERN.

Therefore, the reflection losses with the same phase and reverse phase, $\dot{S}^e$ and $\dot{S}^o$, using the $\dot{S}_{TE}$ and $\dot{S}_{TM}$, are given as:

$$\dot{S}^e = \frac{\dot{S}_{TE} + \dot{S}_{TM}}{2} \quad (20)$$

$$\dot{S}^o = \frac{\dot{S}_{TE} - \dot{S}_{TM}}{2} \quad (21)$$

Using these equations, the reflection loss for a single layer microwave absorber was theoretically calculated. However, the reflection loss for strip and pattern structure typed microwave absorber (as shown in Fig. 3) could not be calculated using these theories but could be calculated by using modified FDTD.

Experimental

As a composite material, we used iron powder (coated by Fe_3O_4, made from carbonyl iron, $Fe(CO)_5$) as a magnetic material (hereafter called FE) and TiO_2 powder as a dielectric material (hereafter called TiO_2) and the powders were mixed with ethylene propylene rubber (hereafter called EPDM). The average grain sizes of FE and TiO_2 were 4.0 μm and 0.98 μm, respectively.

FE generally has the lower magnetic permeability than ferrite materials, but it has a good characteristic of microwave absorption more than ferrite, especially above 4 GHz because it is not affected by Snoke' law [8] and the frequency dispersion of FE is generated on the high frequency side. Because TiO_2 has physical and chemical stability, it can make up for faults in the FE by mixing TiO_2 and FE, for example heavy weight and easy to oxidize. EPDM, used as a holding material, is a no loss resin which is superior to resist oil, heat, ultraviolet rays and water-resistant [9].

In order to know the characteristic of the composite materials, we divided the composite materials by Fe/TiO_2 weight fraction ratio that the predominant property was changed from a magnetic material (FE/TiO_2 = 100/0) to a dielectric material (FE/TiO_2 = 0/100). The fill ratio was 90.9% FE/TiO_2 and the remaining 9.1% was the EPDM.

As shown schematically in Fig. 1(a), we used the coaxial wave guide of a S-parameter method (hereafter called the 7D method). A toroidal-shaped specimen which could be inserted in a type 7D sample holder for ε_r^* and μ_r^* measurements was set in a coaxial sample holder with outer and inner diameters of 7 mm and 1 mm, respectively. For ε_r^* and μ_r^* measurements of a sample using a network analyzer (Wiltron Co. 37269A), an open-short-load (OSL) method was performed in the range from 1 GHz to 18 GHz, for calibration.

Reflection loss, Γ_{11}, in free space was measured using a measurement system shown in Fig. 4, in which the diameter of the arch was 1.5 m, satisfying the condition for far-field, $R \geq 2D^2/\lambda$, where D is the opening size of the antenna, R is the distance between the transmitting

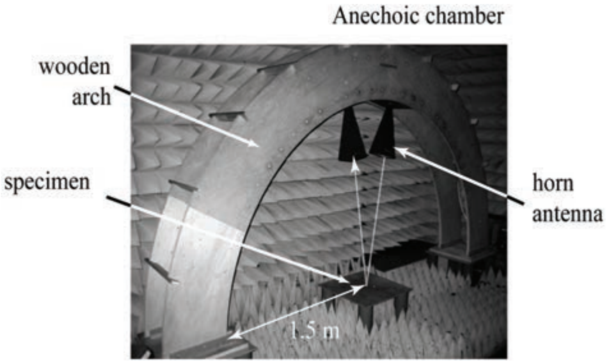

Fig. 4. Experimental set up for reflection loss in a free space.

Table 1. Complex permittivity, ε_r* and complex permeability, μ_r* at 5.8 GHz with changing FE/TI weight ratio

FE/TI Weight ratio (%)	ε_r* and μ_r* at 5.8 GHz (Central frequency of ETC)			
	ε_r'	ε_r"	μ_r'	μ_r"
100/0	15.671	1.009	2.398	1.871
70/30	14.851	1.267	1.953	0.812
60/40	13.928	1.118	1.751	0.601
50/50	12.696	0.991	1.585	0.445
40/60	11.505	0.874	1.476	0.342
20/80	10.034	0.634	1.193	0.132
0/100	8.242	0.573	1.007	0.040

and receiving antennas, and λ is the wavelength. The measurements ware performed using a network analyzer (Wiltron Co. 370B) with a time-domain function in an anechoic chamber to reduce the influence of unnecessary electromagnetic waves from the surrounding reflection body. Measurement of the incident angle dependence of the TE, TM and CP waves was performed by attaching the transmitting and receiving antennas at intervals of 5^o in the supporting wooden arch. For the measurement of TE and TM waves, the direction of the opening of the horn antenna was rotated by 90^o. For the CP wave, the experiment was performed using spiral horn antennas with a clockwise direction for the transmitting antenna and an anti-clockwise direction for the receiving antenna. The reflection loss was measured with the same phase, $\dot{S}^e$. The values of reflection loss for samples were measured by the difference between the reflection loss of a metallic board of the same size and the sample with the metallic board placed as a backing.

As shown in Fig. 3(a), the sample for reflection loss, Γ_{11}, in a free space was formed in a square shape with dimensions of length×width×thickness = 500 mm×500 mm×2.30 mm (hereafter called ALL). In addition to know execution related microwave absorber for an improved ETC system without a characteristic deterioration, as shown in Fig. 3(b), a strip-shaped structure (length×width×thickness = 500 mm 100 mm×2.30 mm, hereafter called the STRIP) and as shown in Fig. 3(c), a pattern structure (length×width ×thickness = 100 mm×100 mm×2.30 mm, hereafter called the PATTERN) sample were measured by a free space method, with separated space intervals of 5, 10, 15, 20, 25, 30 and 40 mm on the metallic board (microwave reflector) with the same size (500 mm×500 mm).

Results and Discussion

Table 1 shows ε_r', ε_r", μ_r' and μ_r" at 5.8 GHz (the central frequency of ETC use in Japan) with changing FE/TiO_2 weight ratio from a magnetic material (FE/TiO_2 = 100/0) to a dielectric material (FE/TiO_2 = 0/100) using the 7D method. As the weight of FE decreases and the weight of TiO_2 increases in the composite materials, in proportion as ε_r', μ_r' and μ_r" gradually decreased. In particular, although FE/TiO_2 = 100/0 is a magnetic material, the complex permittivity real part, ε_r', of it is the highest value of the samples. It seems that Fe_3O_4 , a thin dielectric material covering the FE surface, increases the dielectric constants to appear as a BL (Barrier-Layer dielectrics) condenser which is connected in a series or parallel condenser mechanism [10, 11].

Table 2 shows the reflection loss and central frequency when the reflection loss is the maximum value with changing FE/TiO_2 weight ratio from a magnetic material (FE/TiO_2 = 100/0) to a dielectric material (FE/TiO_2 = 0/100). In Table 2, (a) are calculated values from Eqs. (1)-(11), of complex permittivity, ε_r* and permeability, μ_r*, and (b) are experimental values using the 7D method. As the FE weight decreases and the TiO_2 weight increases, in proportion the central frequencies move to the high frequency range and the reflection losses are gradually decreased. In the results, the central frequencies give theoretical values 4.09-10.40 GHz and experimental values 3.71~13.52 GHz, and reflection losses give theoretical values −29.62~−7.34 dB and experimental values −30.03~ −4.74 dB. Both theoretical and experimental results show fairly good agreement, and it is Fe/TiO_2 = 60/40 that satisfies the necessary condition of a central frequency of 5.8 GHz and reflection loss of −20 dB for ETC use in Japan, especially.

Figure 5 provides the experimental results for reflection

Table 2. Central frequency and reflection loss in the sample with changing volume fraction of Fe/Ti (a) Calculated and (b) Experimental values

FE/TI Weight ratio (%)	(a) Calculated		(b) Experimental	
	Central Freq' [GHz]	Reflection Loss [dB]	Central Freq' [GHz]	Reflection Loss [dB]
100/0	4.09	−29.62	3.71	−30.03
70/30	5.14	−24.50	5.17	−23.78
60/40	5.84	−21.58	5.80	−21.70
50/50	6.41	−18.41	6.65	−17.95
40/60	6.80	−15.96	6.99	−14.84
20/80	8.97	−9.57	8.74	−8.17
0/100	10.40	−7.34	13.52	−4.74

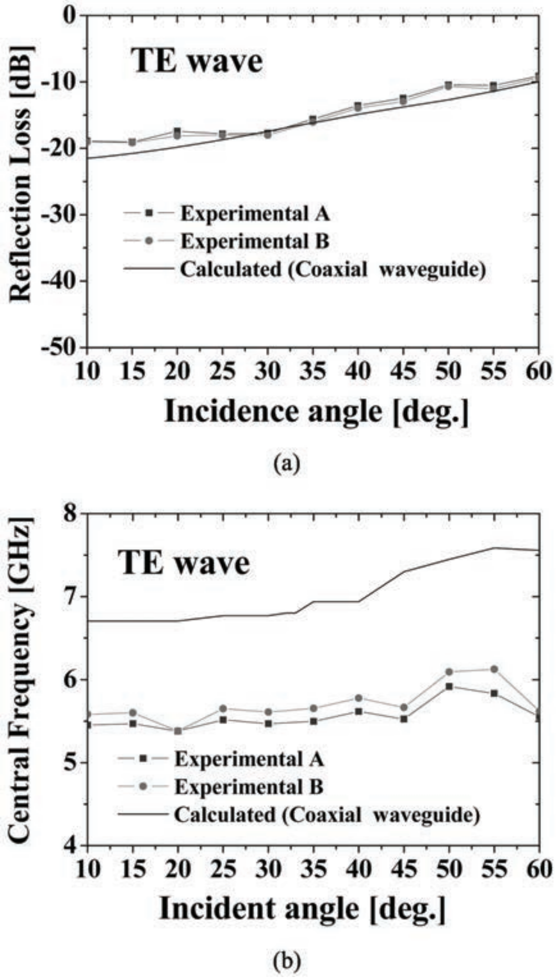

Fig. 5. Experimental and theoretical results for (a) reflection loss, Γ_{11}, and (b) central frequency, fc, of FE/TI = 60/40, incident angles from 10° to 60°, for the TE wave.

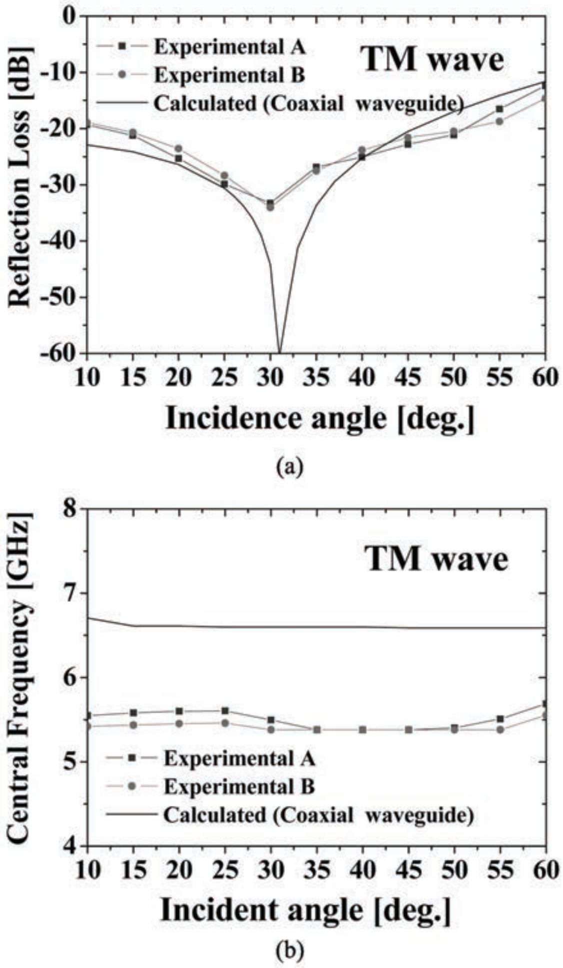

Fig. 6. Experimental and theoretical results for (a) reflection loss, Γ_{11}, and (b) central frequency, fc, of FE/TI = 60/40, incident angles from 10° to 60°, for the TM wave.

loss, which show the maximum value at a central frequency, and the central frequency as a function of the incident angle of FE/TiO_2 = 60/40 for the TE wave and theoretical results estimated from Eqs. (12)-(14). Experimental A is an extension direction of a rubber sample and experimental B is a vertical direction of an extension rubber sample. The reflection losses decrease monotonically with increasing incident angle and both experimental and theoretical results show fairly good agreement. The central frequency moved slightly to a higher frequency and the difference between experimental and theoretical results became approximately 1.1 GHz.

Figure 6 gives the experimental results for the reflection loss for the TM wave, including theoretical values estimated from Eqs. (12)-(16). The theoretical reflection loss shows a maximum at an incident angle of 31°, because the reflection coefficient becomes zero at a certain angle that is determined by the combination of ε_r* and μ_r*, known as the Brewster angle. On the other hand, the experimental values indicating maximum reflection losses around the incident angle of 30° in both A and B directions, where the incident angle in the experiment was changed at intervals of 5° and theoretical values were calculated at intervals of 1°. The central frequency was not dependent on the incident angle and was almost constant for both experimental and theoretical results. The theoretical value was about 1.1 GHz higher than the experimental values.

Figure 7 shows the experimental results for the reflection loss for the CP wave and theoretical values estimated from Eqs. (17)-(21). The reflection loss, $\dot{S}^e$, for the theoretical results increased gradually and experimental results are constant around −20 dB or more. The central frequency moved slightly to a higher frequency and revealed a fairly good agreement with the theoretical value, although a maximum difference of 0.6 GHz arose at incident angles from 10° to 60°. In the results, most of the reflection losses obtained were −20 dB or more and the central frequencies were at 5.8 GHz that satisfies the necessary conditions for ETC use in Japan.

Figure 8 provides the experimental results at 5.8 GHz which is the actual frequency for ETC use for the reflection loss for the CP wave of STRIP and PATTERN structures. Figure 8(a) shows the STRIP A direction in which an incident wave and reflection wave go directly with the

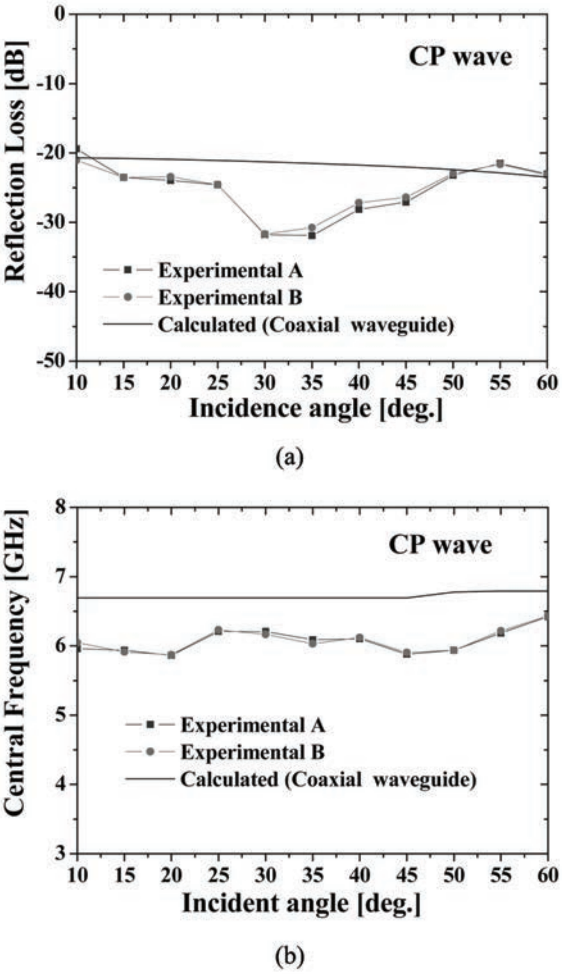

Fig. 7. Experimental and theoretical results for (a) reflection loss, Γ_{11} , and (b) central frequency, fc, of FE/TI = 60/40, incident angles from 10° to 60°, for the CP wave.

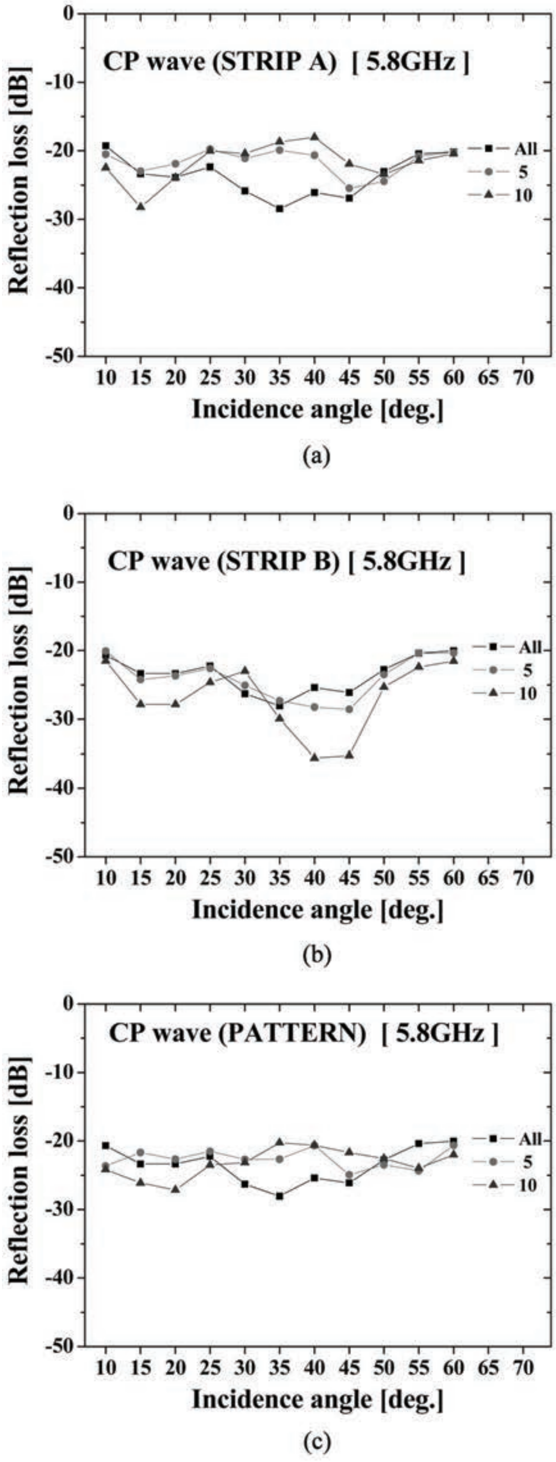

Fig. 8. Experimental results for reflection loss, Γ_{11}, by changing structure (a) STRIP A direction, (b) STRIP B direction and (c) PATTERN structure of FE/TI = 60/40, incident angles from 10° to 60°, for the CP wave at 5.8 GHz (Central frequency of ETC)

strip structure direction. Figure 8(b) shows the STRIP B direction in which an incident wave and reflection wave go directly with the space interval direction. Figure 8(c) shows the PATTERN structure. As the separated space interval increases from 5 mm to 10 mm, reflection losses of the STRIP and PATTERN structures were above –20 dB or more and most of these are much better than uniform structure (ALL) at most of incident angles. In the results, when the separated space interval is within 10 mm, the changing structures of STRIP and PATTERN also satisfied the necessary conditions for ETC use in Japan.

Conclusions

Based on microwave absorber theory, composites of various dielectric (titanium oxide, TiO_2) and magnetic (iron, coated by Fe_3O_4), made from carbonyl iron, Fe $(CO)_5$) materials were evaluated for use in an ETC device. By changing the weight ratio of Fe/TiO_2 in the composite materials (Fe/TiO_2 = 100/0-0/100), we change the values of complex permittivity ($\varepsilon_r^* = \varepsilon_r' - j\varepsilon_r''$) and complex permeability ($\mu_r^* = \mu_r' - j\mu_r''$), and the results are applied in the design of a microwave absorber which matches the reflection losses and the central frequency for a specific purpose.

It is Fe/TiO_2=60/40 that satisfied the necessary conditions of a central frequency 5.8 GHz and reflection loss of –20 dB or more around for ETC use in Japan, in both theoretical and experimental results. We evaluated the reflection losses using TE wave, TM wave and CP wave in a free space. The CP wave, actually used in ETC, was –20 dB or more around a central frequency of 5.8 GHz for incident angles from 10^o to 60^o. Also we show that changing the structure of STRIP and PATTERN also satisfied the necessary conditions for ETC use in Japan when the separated space interval is within 10 mm.

References

1. Y. Shimizu, I. Sugiura, K. Ishino and T. Inui: Nikkei Tech. Book, (1999) [in Japanese].
2. Japanese Ministry of Land: Report for Development for ETC Related Technology (2004) [in Japanese]
3. k. Kashihara, N. Fujita, H. Hashimoto, Y. Ijiri, K. Hosotani, T. Mitsui and T. Kudo: Mitsubishi Cable Industries Review, Vol. 99, (2002) pp. 69-77 [in Japanese]
4.. M. Nicolson and G.F. Ross: IEEE. Trans. Instrum. Meas, Vol. IM-19, No. 4, (1970) pp. 377-382.
5. J. Baker, E.J. Vanzura and W.A. Kissick: IEEE. Trans. Microwave Theory Tech, Vol. 38, No. 8, (1990) pp. 1096-1103.
6. K. Hatakeyama, M. Hosokawa, Y. Sakai, H. Togaya and K. Yamaguchi: EMCJ-102, pp. 85-90 (2001-12) [in Japanese]
7. K. Kashihara, N. Fujita, H. Hashimoto, Y. Ijiri, K. Hosotani, T. Mitsui, and T. Kudo: Mitsubishi Cable Industries Review, Vol. 99, (2002) pp. 69-77 [in Japanese]
8. J.L. Snoek: Physica, Vol.14, (1948) pp.207-217.
9. M. Saito, T. Yamamoto, T. Sakamoto, H. Niori, M. Chino and M. Kobayashi: Ferroelectrics, Vol. 263, (2000) pp. 9-12 [in Japanese]
10. N. Yamaoka and T. Matsui: Grain Boundary Phenomena in Electronic Ceramics Vol. 1, Amer. Ceram. Soc. Inc, (1980) pp. 232-241.
11. H.D. Park and D.A. Payne: Grain Boundary Phenomena in Electronic Ceramics Vol. 1, Amer. Ceram. Soc. Inc, (1980) pp. 242-253.